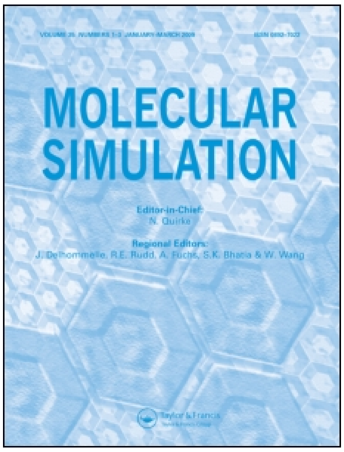

Molecular Simulation
Publication details, including instructions for authors and subscription information:
http://www.informaworld.com/smpp/title~content=t713644482

Monte Carlo Simulations of N_2 and O_2 Adsorption in Silicalite and CaLSX Zeolites

Caroline Mellot[a]; Jean Lignieres[a]
[a] AIR LIQUIDE, Centre de Recherche Claude Delorme, Les Loges-en-Josas, Jouy-en-Josas, France

To cite this Article Mellot, Caroline and Lignieres, Jean(1997) 'Monte Carlo Simulations of N_2 and O_2 Adsorption in Silicalite and CaLSX Zeolites', Molecular Simulation, 18: 6, 349 — 365

To link to this Article: DOI: 10.1080/08927029708024130

URL: http://dx.doi.org/10.1080/08927029708024130

Molecular Simulation, 1997, Vol. 18, pp. 349–365
Reprints available directly from the publisher
Photocopying permitted by license only

MONTE CARLO SIMULATIONS OF N_2 AND O_2 ADSORPTION IN SILICALITE AND CaLSX ZEOLITES

CAROLINE MELLOT and JEAN LIGNIERES

AIR LIQUIDE, Centre de Recherche Claude Delorme, Les Loges-en-Josas,
B. P. 126, 78350 Jouy-en-Josas, France

(Received July 1996; accepted August 1996)

Grand Canonical Monte Carlo simulations are performed with two different zeotype structures, silicalite and CaLSX, chosen for their different adsorption and separation properties toward N_2 and O_2 at ambiant temperature and pressure. The purpose of this work is to obtain from GCMC simulations a consistent approach to N_2 and O_2 adsorption in both structures, especially when compared to experimental data. This study investigates how far a simple model including a Lennard-Jones term and a coulombic term for electrostatic interactions is able to provide a significant description of the zeolite-sorbate system, using a minimum of adjustable parameters. Silicalite adsorption properties are well captured by the simulations as no N_2/O_2 selectivity is obtained. Energy distribution density grids show that the silicalite structure provides an homogeneous surface toward N_2 and O_2 molecules and induces no energetic discrimination between both sorbates. The CaLSX zeolite provides a highly heterogeneous surface toward N_2 molecules owing to the interaction of the quadrupolar N_2 molecules with the electric field gradient generated by the extraframework cations. The simulations, while failing in capturing the experimental N_2 isotherm in the whole [0–1] bar pressure range, clearly show that the high N_2/O_2 selectivity is correlated to the distribution of the Ca^{2+} cations over the sites S_{II} of the supercages.

Keywords: GCMC simulations; adsorption; zeolite; nitrogen; oxygen; silicalite; CaLSX

INTRODUCTION

Classical cryogenic processes for the separation of oxygen and nitrogen from air are gradually giving way to a new generation of technologies involving either Pressure Swing Adsorption (PSA) and Vacuum Swing Adsorption (VSA) processes or polymeric membranes permeation processes. The VSA technology is now largely used for O_2 production, supplying an enriched stream containing up to 95% of O_2 for a variety of applications in the steel industry, enhanced combustion, soil and wastewater cleanup, or paper-bleaching. The basic principle of O_2 production from air by PSA/VSA processes relies on the selective adsorption of N_2 over O_2 in a zeolitic adsorbent bed at room temperature. The VSA process consists of adsorption-desorption steps operating between a high pressure, for the production of the O_2 enriched stream, and a lower pressure, for the adsorbent regeneration step. In addition to the operating parameters of the process itself, one of the important factors influencing the performance of the production unit is related to the adsorption properties of the zeolitic material at thermodynamic equilibrium. The physico-chemical properties of the zeolitic material strongly determine the shape of both the N_2 and O_2 isotherms, especially in terms of N_2/O_2 selectivities at the production pressure (~ 1 bar). A thorough understanding of the dependance of adsorption isotherms upon the microscopic features of the zeolite is therefore of prime importance.

The separation of N_2 and O_2 is performed in cation-containing zeolites. When considering N_2 and O_2 molecular properties (Tab. I), the significantly higher permanent quadrupole moment of N_2 compared to that of O_2 is the main cause of their thermodynamic separation, as N_2 interacts more strongly than O_2 with the field gradient generated by the extra-framework cations. In fact, the combination of a large variety of framework structures and of their different cationic-exchanged forms leads to a large diversity of adsorption and separation properties. Figure 1 is an attempt to illustrate this latter point, showing the schematic features of pure N_2 and O_2 adsorption isotherms in different zeolitic structures, presenting N_2/O_2 selectivities as the ratio of adsorbed quantities of N_2 over O_2 at 1 bar. Purely siliceous silicalite is a representative example of a zeotype material without any N_2/O_2 selectivity, which is attributed to the lack of extra-framework cations in this material. When considering cation-containing structures such as X-type zeolites, separation effects are observed. The as-synthetized NaX zeolite is characterized by a N_2/O_2 selectivity of 3 at 1 bar. The exchanged CaX zeolite is characterized by a clear increase in N_2/O_2 selectivity, up to 4 at 1 bar, which can be explained by the stronger interaction of N_2 molecules with divalent cations. Nevertheless, the simple difference in physical properties between N_2 and O_2 molecules, while explaining the separation effect in its basic principle, does not provide the basis for a systematic correlation between the structural and chemical features of a specific zeolite and its separation performances in terms of N_2/O_2 selectivity at ambiant pressure.

The use of simulations is therefore of special interest in order to investigate this correlation, furnishing the link between microscopic phenomena and macroscopic properties. In that respect, molecular modeling has recently

TABLE I Molecular properties of nitrogen and oxygen

	Lennard-Jones $\sigma(\mathring{A})$	$\varepsilon/k(K)$	*Polarizability* $\alpha(10^{-24}cm^3)$	*Quadrupole Moment* $Q(10^{-40}C.m^2)$
O_2	3.467	106.7	1.58	−1.3
N_2	3.798	71.4	1.74	−4.7

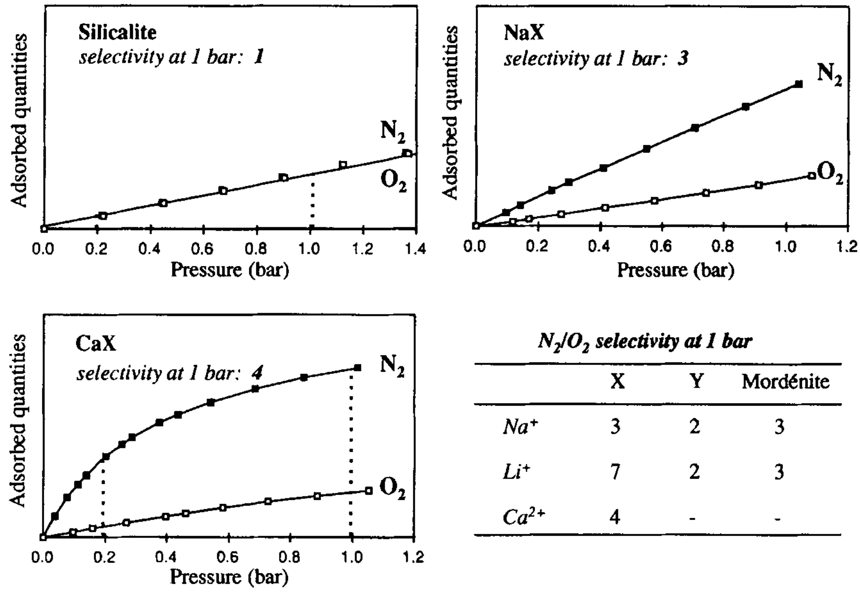

N_2/O_2 selectivity at 1 bar

	X	Y	Mordénite
Na^+	3	2	3
Li^+	7	2	3
Ca^{2+}	4	-	-

FIGURE 1 Schematic features of nitrogen and oxygen adsorption isotherms in different zeotype structures at ambient temperature.

emerged as an efficient tool for improving the fundamental understanding of basic microscopic phenomena and for helping to solve industrially relevant problems involving chemical or physico-chemical processes. When dealing with complex molecular systems like zeolites, experimental studies have preceeded by far the theoretical ones. Yet, as programming technologies improve and computational power increases, simulation methods are being increasingly used as a complement to experiment. A molecular modeling approach enhances the fundamental understanding of the basic microscopic phenomena and gives a better insight into interactions at a molecular level, especially into the behaviour of the adsorbed phase at the solid-gas interface. As the separation mechanism is determined by molecular-level interactions, Grand

Canonical Monte Carlo (GCMC) simulations are appropriate for correlating the microscopic features of the zeolite/sorbate system with macroscopic properties of interest that are experimentally determined such as adsorption isotherms and isosteric heats.

In the following, GCMC simulations are used to study the single-component adsorption properties of two different structures, silicalite, the purely siliceous form of the ZSM-5 zeolite, and CaLSX, the fully calcium exchanged form of the LSX faujasite-type zeolite ($Si/Al = 1$). Both zeolites have known crystalline structures, and differ by their Si/Al ratio and their cationic composition. Simulating adsorption properties of both structures is of special interest as silicalite has no N_2/O_2 selectivity while the CaLSX zeolite has a high N_2/O_2 selectivity at 1 bar.

A large range of studies of single-gas adsorption in microporous sorbents by Monte-Carlo or Molecular Dynamics is available in the literature [1], and is mainly devoted to the improvement of the theoretical description of physisorption and to the development of accurate interaction models, in order to have a description as wide and precise as possible of the sorbate/sorbent system properties. Our purpose here is to obtain from the GCMC simulations a significant approach to N_2 and O_2 adsorption, especially when compared to experimental data, through the use of a simple model that may be easily transferred to any zeolitic structure. Adsorption properties, and more especially N_2/O_2 selectivities, are simulated in a restricted range of pressure (up to 1 bar) and temperature (298 K). This work investigates how far a simple repulsion-dispersion model coupled with the electrostatic interactions described by point charges is able to provide a significant description of the zeolite-sorbate system, using a minimum of adjustable parameters. Calculations were performed using the Biosym software package (Biosym Technologies Inc., San Diego, 1994, release 237). As no specific forcefield for (N_2, O_2/zeolite) system is implemented in the Biosym software, the different forcefield parameters were estimated on both zeolites. In a first step, adsorption of N_2 and O_2 in the purely siliceous, therefore cation-free, silicalite zeotype material was simulated in order to obtain the forcefield parameters describing the interactions involved between N_2/O_2 molecules and the oxygen atoms of the framework. In a second step, GCMC simulations were investigated on the cationic CaLSX zeolite, starting with the previously determined forcefield parameters. The test of the ability of the simulations to predict the adsorption properties of both microporous structures is discussed in a comparison with experimental N_2/O_2 selectivities and isotherms.

INTERACTION MODEL FOR N_2 AND O_2 ADSORPTION IN ZEOLITES

When considering the simulation of adsorption isotherms in zeolites, the two critical steps in the GCMC calculations are the choice of the structural model for the zeolite and the choice of the interaction model describing sorbate/sorbent and sorbate/sorbate interactions. Once a full structural representation of the zeolite is fixed, the success of an attempt at modeling sorption properties relies essentially on the potential function describing the interactions involved in the sorbent-sorbate system. The validity of a GCMC calculation has then to be established in comparison with experiment (isosteric heats, isotherms, Henry's constant), as it is certainly the best test of the assumptions regarding the intermolecular interactions.

Considering the sorbent-sorbate system, the total intermolecular interaction energy may be expressed as follows:

$$E_{\text{total}} = E_{\text{dispersion-repulsion}} + E_{\text{electrostatic}} + E_{\text{induction}} \tag{1}$$

The repulsion-dispersion contribution is always present and belongs to the non-specific part of the interaction. The dispersive interaction results from the interaction between two instantaneous dipoles and is generally described as a function of the polarizabilities of the interacting atoms. The electrostatic term includes coulombic type interactions, or more generally, multipole-multipole interactions. The induction energy term, often distinguished from other electrostatic contributions while being of an electrostatic nature, results from the distorsion of the molecule under the influence of the external electric field. The strength of this interaction is directly related to the atomic polarizabilities of the interacting species and to the strength of the external electric field gradient generated by the extraframework cations.

As a first approximation, the inductive part of the interaction is deliberately neglected in the interaction model. When considering N_2/O_2 separation in a cationic zeolite, the neglect of induction energy may at first be justifiable as the N_2 and O_2 atomic polarizabilities are very similar. The inductive interaction between sorbed molecules and cations is consequently of a non-specific nature and gives rise to no separation effect. This approximation is in agreement with recent DFT calculations [2] and may be used here considering that the zeolitic framework induces an important screening of the electric field generated by the highly inductive extraframework cations.

In this work, the total energy is therefore taken as the sum of a repulsion-dispersion term and a coulombic term. For the repulsion-dispersion term, the Lennard-Jones potential expression is used:

$$E_{ij}=\frac{A_{ij}}{r_{ij}^{12}}-\frac{B_{ij}}{r_{ij}^{6}}=\varepsilon_{ij}\left[\left(\frac{r^*_{ij}}{r_{ij}}\right)^{12}-2\left(\frac{r^*_{ij}}{r_{ij}}\right)^{6}\right] \tag{2}$$

where A_{ij} is the repulsion constant and B_{ij}, the dispersion constant, with $\varepsilon_{ij}=B_{ij}^{2}/4A_{ij}$, $\sigma_{ij}=(A_{ij}/B_{ij})^{1/6}$ and $r^*_{ij}=2^{1/6}\sigma_{ij}$. This potential considers interactions between pairs of atoms and is often referred to as an atom-atom potential. A knowledge of the parameters (A_{ij}, B_{ij}) or $(r^*_{ij}, \varepsilon_{ij})$ sets for each interacting pair is therefore required. The equilibrium separation distance r^*_{ij} of the interacting pair is expressed as the sum of the van der Waals or ionic radii of the interacting atoms (r_i and r_j):

$$r^*_{ij}=(r^*_{ii}+r^*_{jj})/2 \text{ with } r^*_{ii}=2r_i \tag{3}$$

Concerning the dispersive interaction, there are three commonly used expressions for the estimation of the attractive constant, B_{ij}, which all may be summarized by the following formula:

$$B_{ij}=K\alpha_i\alpha_j/(\beta_i+\beta_j) \tag{4}$$

with three different ways of defining the β term according to London [3a]($\beta=1/E_i$), Slater-Kirkwood [3b]($\beta=(\alpha/n)^{1/2}$), or Kirkwood-Müller [3c]($\beta=\alpha/\chi$), where E_i is the ionization potential, α the polarizability, n the number of electrons in outer shells, and χ the magnetic susceptibility. The variety of formulations of the dispersion constant, B_{ij}, is a barrier to the development of a quantitative theoretical approach to the *a priori* calculation of adsorption energies. Nevertheless, the problem may be avoided if the development of the forcefield is based on the adjustment of the ε_{ij} parameters, using a mixing rule from both formula (3) and (4):

$$\varepsilon_{ij}=\sqrt{\varepsilon_{ii}\varepsilon_{jj}}\,\frac{(r^*_{ij})^3(r^*_{ij})^3}{(r^*_{ij})^6}\cdot\frac{2(\beta_i\beta_j)^{1/2}}{(\beta_i+\beta_j)} \tag{5}$$

It is interesting to notice that when both conditions $r^*_{ii}\sim r^*_{jj}$ and $\beta_i\sim\beta_j$ are fulfilled, the commonly used mixing rule $\varepsilon_{ij}=(\varepsilon_i\varepsilon_j)^{1/2}$ is obtained. Considering the interactions of CH_4, N_2, Ar and O_2 with oxygen atoms O_z of the zeolitic framework, it can be easily shown that the β term may be taken as equal to 1, whatever the choice of the B_{ij} formula is (For example, $\beta_{Ar-Oz} = 0.997$ according to the $\beta = 1/E_i$ expression of London).

A further classical reduction of the number of adjustable parameters consists of neglecting the repulsive and dispersive contributions of silicon and aluminum atoms, as they are screened by the oxygen atoms of the framework. As a matter of fact, the accessible part of the framework towards sorbed molecules consists mainly of oxygen atoms. Furthermore, the low polarizabilities of T(Si, Al) atoms in comparison with that of oxygen atoms of the framework suggest that negligible Lennard-Jones interactions are involved between adsorbed N_2 or O_2 molecules and T atoms. Consequently, the repulsive-dispersive contribution of the zeolite may be assigned exclusively to oxygens of the framework and cations. Nevertheless, this assumption implies that the influence of Si and Al atoms on the dispersion-repulsion interactions will be included in the fitting of ε_{ij} parameters of oxygens of the framework.

The electrostatic interaction is estimated using the following classical expression:

$$E = \sum_{i,j} \frac{q_i q_j}{r_{ij}} \tag{6}$$

The zeolite is described as a semi-ionic structure and the partial charges are taken as follows: Si(+2.4), O(−1.2), Al(+1.4) and Ca(+2). The quadrupole moments of N_2 and O_2 are described by a three point charge model. The two outer sites are separated by a distance l(1.2 Å for O_2, 1.1 Å for N_2) and have a charge $-q(-0.112$ for $O_2)$ and $(-0.486$ for $N_2)$. The third midpoint site has a charge $+2q$. Charges are chosen in order to fit the experimental quadruple moments [4] of the nitrogen molecule, $4.7.10^{-40}$ C.m^2, and the oxygen molecule, $1.3.10^{-40}$ C.m^2. An Ewald summation is used for calculating electrostatic interactions.

ADSORPTION OF METHANE, OXYGEN AND NITROGEN IN SILICALITE

The silicalite structure is considered in its orthorombic form with $a = 20.02$ Å, $b = 19.89$ Å and $c = 13.38$ Å [5]. The microporous network is made of two different types of channels, both delineated by 10-member-rings. A set of straight channels runs in the direction of the (010) axis and a second set of sinusoidal channels intersects the straight channels and runs in the direction of the (100) axis. GCMC calculations were performed on a 2 × 2 × 2 replicated unit-cell.

The calculations require a knowledge of the dispersive interactions of oxygens of the framework with methane ($\varepsilon_{OZ\text{-}CH4}$), nitrogen ($\varepsilon_{OZ\text{-}N}$), oxygen ($\varepsilon_{OZ\text{-}O}$) and argon ($\varepsilon_{OZ\text{-}Ar}$) molecules. Concerning methane, the $\varepsilon_{OZ\text{-}CH4}$ parameter is taken from a study [6] of a spherical model for methane in silicalite using potential parameters that were adjusted to reproduce the experimental adsorption heat and Henry's constant at 298 K [7]. We then deduced the ε_{OZ} parameter from $\varepsilon_{OZ\text{-}CH4}$, r^*_{CH4} and r^*_{OZ}, using the mixing rule (5). A knowledge of ε_{OZ} therefore allows the extention of the forcefield to the $\varepsilon_{OZ\text{-}i}$ parameters for $i = \mathrm{Ar}$, $i = \mathrm{N(N_2)}$ and $i = \mathrm{O(O_2)}$, using the mixing rule (5) in a similar way and the $\varepsilon_{N(N2)}$, $\varepsilon_{O(O2)}$ and ε_{Ar} parameters from liquids [8,9]. Table II summarizes the different potential parameters obtained. Table III reports the results of the GCMC calculations performed at 0.2 bar and 298 K, for N_2, O_2 and Ar adsorption in the silicalite structure. In each case, the isosteric heat of adsorption and the Henry constant are reported. Despite the underestimation of adsorption enthalpies, good simulations of N_2, O_2 and Ar adsorption are obtained, especially as no selectivity of adsorption between N_2, O_2 and Ar is found. Figure 2 shows the energy distributions of N_2 and O_2 in silicalite, represented as the number of grid points of the 2 × 2 × 2 replicated unit-cell having accepted configurations of energy E_i as a function of E_i. It is noticeable that we obtain very similar distributions in both cases, centered around $E_1 = -10.2\,\mathrm{kJ.mol^{-1}}$ and $E_2 = -13.2\,\mathrm{kJ.mol^{-1}}$ in the case of N_2 adsorption, and around $E_1 = -10\,\mathrm{kJ.mol^{-1}}$ and $E_2 = -12.5\,\mathrm{kJ.mol^{-1}}$ in the case of O_2 adsorption.

Figure 3 shows the spatial distribution of N_2 molecules in silicalite for $E_1 = -10.2\,\mathrm{kJ.mol^{-1}}$ (3a) and $E_2 = -13.2\,\mathrm{kJ.mol^{-1}}$ (3b). Adsorbed N_2 molecules are uniformly distributed over the microporous structure, over straight and sinusoidal channels and intersections. A selection among most energetic configurations (Fig. 3b) shows that local minima of the potential

TABLE II Pair potential parameters used for CH_4, Ar, $O(O_2)$, $N(N_2)$ and O(zeolite) in GCMC calculations

		CH_4^6	Ar^{10}	$O(O_2)^{11}$	$N(N_2)^{14}$	$O(zeolite)$
r_{ii}	(Å)	4.187	3.820	3.468	3.724	3.040
ε_{ii}/k_B	(K)	147.95	119.80	44.50	36.40	139.96
$r^*_{OZ\text{-}i}$	(Å)	3.613	3.430	3.254	3.382	
$\varepsilon_{OZ\text{-}i}/k_B$	(K)	133.30	124.53	77.90	69.21	

TABLE III Adsorption of methane in silicalite at 0.2 bar and $T = 298$ K

	N(cal) *molec/uc*	K_H*(calc)* *mol/uc/atm*	K_H*(exp)* *mol/uc/atm*	ΔH*(calc)* *kJ.mol*$^{-1}$	ΔH*(exp)* *kJ.mol*$^{-1}$
N_2	0.23	1.13	0.98[12]	−14.40	15.1 ± 1.4[12]
O_2	0.22	1.11	1.14[14]	−14.14	–
Ar	0.26	1.32	0.89[12]	−14.32	16 ± 0.9[13]
CH_4	0.85	4.30	5.3[7] – 3.4[7]	−18.31	20[7]

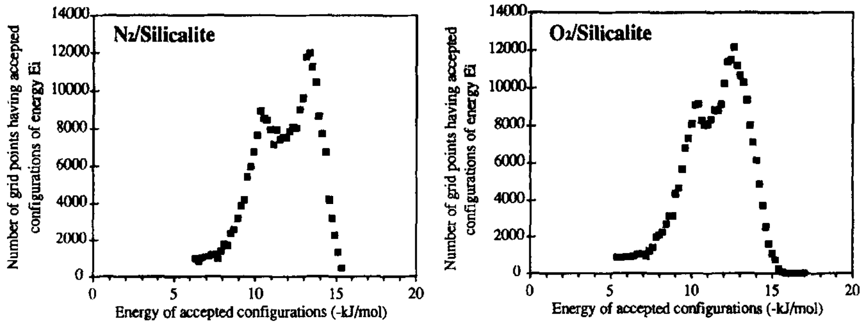

FIGURE 2 Energy distribution of accepted configurations for N_2 and O_2 in silicalite (0.2 bar, 298 K) expressed as the number of grid points having accepted configurations of energy E_i as a function of E_i.

surface are in the confined regions of the sinusoidal and straight channels and at the intersections of both sets of channels. Spatial representation for oxygen and methane adsorption would give similar distributions to that of nitrogen, as sorbate-sorbent interactions are essentially of a dispersive nature. The existence of such local minima in the silicalite structure has already been reported in [6] from the contour plot of the potential energy for a single methane molecule in the silicalite lattice. These high potential regions are interpreted in terms of strong sorbate-sorbent interactions with the "walls" of the zeolite, in the confined regions of straight channels and sinusoidal channels.

These results clearly show that GCMC calculations are successful in simulating no energetic discrimination between O_2 and N_2 adsorption in the silicalite structure. Interactions are essentially of a dispersive nature and electrostatic interactions have no significant contribution. In conclusion, a unique set of (r^*_{ii}, ε_{ii}) parameters for the oxygen atoms of the framework is able to provide a good simulation of silicalite adsorption properties, within a restricted range of pressure and temperature, toward three different sorbate molecules (Ar, O_2 and N_2).

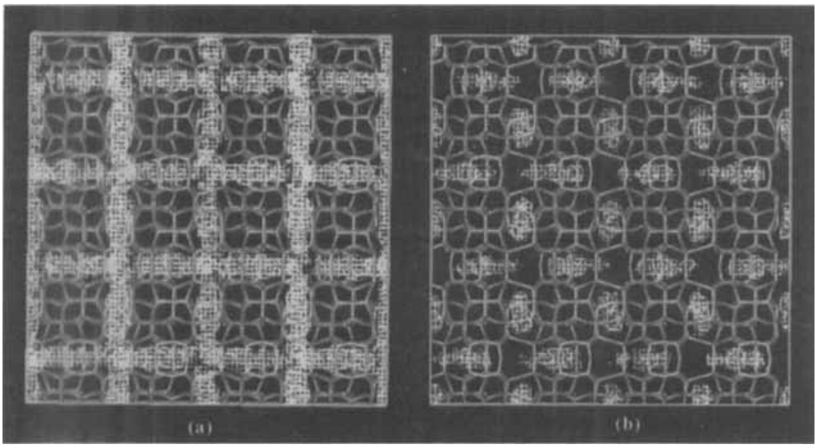

FIGURE 3 Energy distribution density grids for nitrogen in the silicalite channels (0.2 bar, 298 K). (a) Accepted configurations of energy $E_1 = -10.2\,kJ.mol^{-1}$. (b) Accepted configurations of energy $E_2 = -13.2\,kJ.mol^{-1}$.

ADSORPTION OF NITROGEN AND OXYGEN IN CaLSX

As shown in Figure 1, the CaX zeolite is known for its good performances for N_2/O_2 separation, which is at first interpreted by the strong electrostatic interactions of the N_2 molecules with divalent cations. In the following section, the simulation work on silicalite is extended to the study of N_2 and O_2 adsorption in the cation containing structure, CaLSX. For the structure used in the simulations, the GCMC calculations were carried out starting from a recent diffraction refinement of the dehydrated CaLSX zeolite [10]. The chemical composition was taken as follows: $Si_{96}Al_{96}Ca_{48}O_{384}$ per unit-cell. In the LSX structure, the framework has a Si/Al ratio equal to 1, therefore consisting of strictly ordered SiO_4 and AlO_4 tetrahedra. The tetrahedral arrangement of sodalite units linked together by means of hexago nal prisms builds a three-dimensional network of interconnected supercages. The sodalite units and the hexagonal prisms are inaccessible to N_2 and O_2 molecules, while the supercages are accessible to both. The 48 Ca^{2+} cations were distributed as follows: 16 Ca^{2+} cations in sites S_I at the center of hexagonal prisms, and 32 in sites S_{II}, in each 6-ring window of the supercages; both S_I and S_{II} therefore having full-occupancies. As shown in Figure 4, each supercage contains four accessible Ca^{2+} cations symmetri-

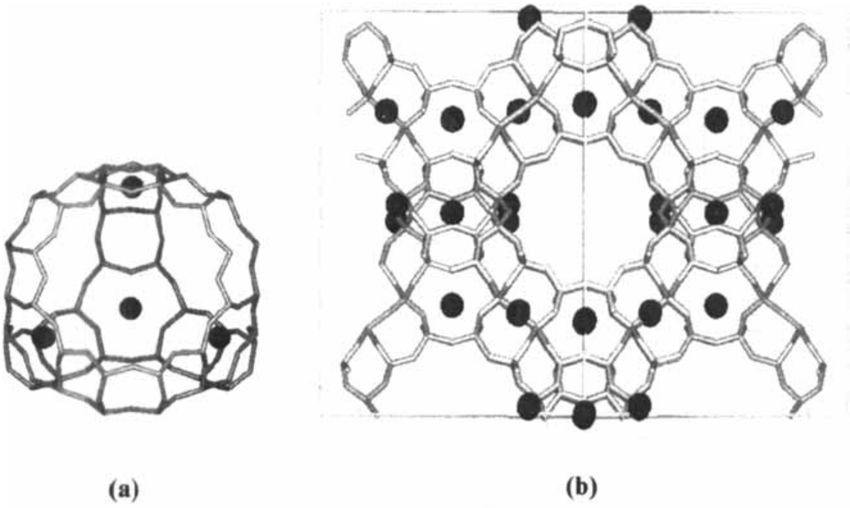

FIGURE 4 (a) Representation of an isolated supercage in the CaLSX zeolite, showing four Ca^{2+} cations distributed over the four sites S_{II}. (b) View of the CaLSX unit-cell.

cally distributed over four S_{II} sites, while the other cations in sites S_I are in confined regions. Experimental data on N_2 and O_2 adsorption in the CaX structure show a N_2/O_2 selectivity around 4 at ambient pressure and temperature, when expressed as the ratio of the adsorbed quantities of N_2 over O_2. The adsorption isotherm for nitrogen is characterized by a strong curvature, while the adsorption isotherm for oxygen has a linear behaviour in the whole [0–1] bar pressure range (see Fig. 5).

In a first step, adsorption of O_2 was simulated starting with the $\varepsilon_{OZ\text{-}O}$ parameter obtained in the previous section on silicalite ($\varepsilon_{OZ\text{-}O} = 77.90\,K$). Concerning the $Ca^{2+}/O(O_2)$ interaction parameters, $r^*_{Ca\text{-}O}$ was calculated from the ionic radius of Ca^{2+} (0.99 Å) and from $r^*_{O\text{-}O} = 3.468$ Å, and $\varepsilon_{Ca\text{-}O}$ was estimated from the London formula ($\varepsilon_{Ca\text{-}O} \sim 85.27\,K$). A first simulation starting from these parameters did not provide a correct fit of the O_2 adsorption isotherm around 1 bar in terms of adsorbed quantities. An increase of 200% of the $\varepsilon_{Ca\text{-}O}$ parameter induced only a small variation on the total adsorption energy ($\sim 0.5\,kJ.mol^{-1}$). As a consequence, an adjustment of the $\varepsilon_{Ca\text{-}O}$ parameter within reasonable values could not provide a correct fit to the experimental isotherm. The different energetic contributions to the total energy were then estimated as follows. For the electrostatic contribution, the interaction of the quadrupole moment of O_2 with the electric field generated by the zeolite structure consists of 15% of the total

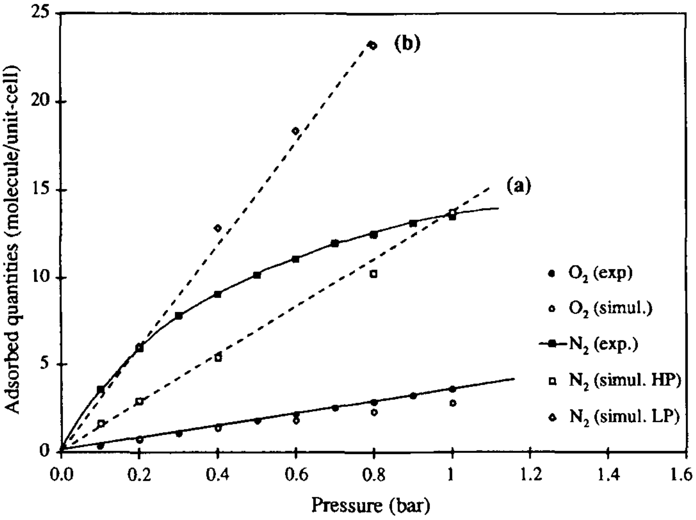

FIGURE 5 Experimental (full lines) and simulated (dashed lines) isotherms for nitrogen and oxygen in the calcium-exchanged X-type zeolite, at 298 K. (a): simulated isotherm obtained for an adjustment in the high pressure region (HP), around 1 bar. (b): simulated isotherm obtained for an adjustment in the low pressure region (LP), around 0.2 bar.

energy. The dispersive contribution emanating from the Ca^{2+} cations is around 10%. The dispersive contribution emanating from the oxygen atoms of the framework is the main contribution and consists of the remaining 75%. A correct fit toward experimental adsorption energy and adsorbed quantities for oxygen was provided in the whole [0–1] bar pressure range by increasing the $\varepsilon_{OZ\text{-}O}$ parameter from 77.9 K to 90 K, leading to an increase of $2.5\,kJ.mol^{-1}$ of the total interaction energy. This step shows that the first $(r^*_{OZ\text{-}O}, \varepsilon_{OZ\text{-}O})$ set of parameters determined from the silicalite adsorption properties cannot be straightforwardly transferred to the CaLSX zeolite. From the increase of the $\varepsilon_{OZ\text{-}O}$ parameter required to fit the experimental isotherm for oxygen, it may be estimated that the polarizability of the framework oxygens in the CaLSX is increased in a ratio of 1.14 in comparison with silicalite. This evolution of oxygen atomic polarizability from silicalite to CaLSX is in agreement with experimental estimations of the polarizability of oxygen atoms in different microporous materials [11, 13], showing that the polarizability is modified by the degree of covalency of the O—(Si, Al) bonds and increases with the ionicity of the structure.

Concerning the simulation of N_2 adsorption, the $\varepsilon_{OZ\text{-}N}$ parameter was deduced from the new ε_{OZ} parameter determined from the simulation of O_2 adsorption and using the mixing rule (3). The remaining adjustable parameters are the repulsive-dispersive parameters for the $Ca^{2+}/N(N_2)$ interaction. Fixing the dispersive parameter using the Kirkwood-Müller formula, the repulsive parameter was adjusted in order to fit correctly the nitrogen adsorption quantity at 1 bar, reproducing therefore the experimental N_2/O_2 selectivity at 1 bar. Figure 5 shows the comparison between experimental and the simulated isotherm (curve a) between 0 and 1 bar.

An analysis of the energy distribution and density grids for N_2 and O_2 adsorbed molecules provides a first insight into the correlation between the selective adsorption properties of the CaLSX zeolite and the nature of sorbate-sorbent interactions. Figure 6 shows the energy distribution curves of N_2 and O_2 molecules, represented as the number of grid points per unit-cell having accepted configurations of energy E_i. The main feature is that energetic distributions for O_2 and N_2 strongly differ from one another. Adsorption energies for N_2 molecules are essentially gathered around $-25\,kJ.mol^{-1}$ and $-18\,kJ.mol^{-1}$, while adsorption energies for O_2 molecules are lower and spread over a wider range. Both curves show, on the one hand, that N_2 is more energetically adsorbed than O_2, and on the other hand that the CaLSX structure behaves like an heterogeneous surface toward N_2 adsorption when compared to that of O_2. A vizualization of the energy distribution density grids of N_2 (Fig. 7a) shows that the most energetically favourable sites ($E_i = -25\,kJ.mol^{-1}$) are gathered in circular rings facing each Ca^{2+} cation in site S_{II}, while all other configurations, represented here down to $-9\,kJ.mol^{-1}$ (Fig. 7b), are spread in other regions of the microporous network. A similar analysis of energy distribution density grids for O_2 molecules would show a uniform distribution of accepted configurations over the zeolite walls, without any localization effects. In the case of

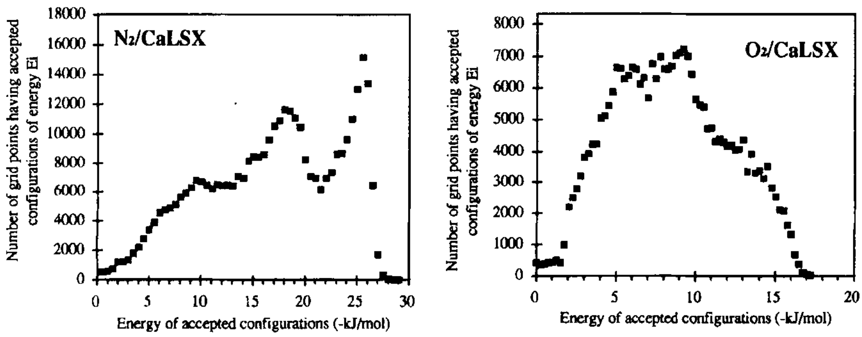

FIGURE 6 Energy distribution of accepted configurations for N_2 and O_2 in the CaLSX zeolite (1 bar, 298 K), expressed as the number of grid points having accepted configurations of energy E_i as a function of E_i.

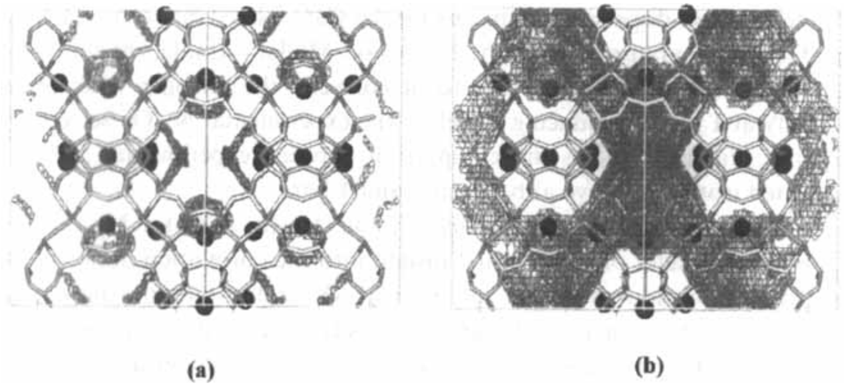

FIGURE 7 Energy distribution density grids for nitrogen in the CaLSX zeolite (1 bar, 298 K). (a) Accepted configurations of energy $E_1 = -25\,\mathrm{kJ.mol}^{-1}$. (b) Accepted configurations of energy $E_2 = -9\,\mathrm{kJ.mol}^{-1}$.

N_2 adsorption, the CaLSX structure provides an energetically heterogeneous surface, with a concentration of favourable positions around the four Ca^{2+} cations of each supercage, as the gradient of the electric field is at its maximum value near the cations. Simulations have been efficient in showing how energetic discrimination is performed between N_2 and O_2 molecules within the microporous structure of the CaLSX zeolite.

Yet, as shown in Figure 5 (curve a), the adjustment of the repulsive interaction in the high pressure region around 1 bar leads to an underestimation of the nitrogen capacity in the whole [0–1] bar pressure range. Similarly, the low pressure part of the isotherm is well simulated when decreasing the repulsive interaction between the cation and the N_2 molecule, leading to an over-estimation of adsorption capacity in the high pressure region. The inability of the parameters of our model to fit the curvature of the nitrogen isotherm in CaLSX raises a more fundamental question related to the nature of adsorption sites in the CaLSX structure. The low pressure region studied here corresponds to very low adsorbed quantities, less than one N_2 molecule per supercage. Assuming an homogeneous distribution of the sorbate molecules within the supercages, no sorbate-sorbate interactions are involved. Calcium cations are the most favourable adsorption sites for N_2 molecules within the supercage. Considering that each supercage contains four Ca^{2+} cations in sites S_{II} and that all of them are equally accessible adsorption sites for N_2 molecules, the loading of one N_2 molecule per supercage is far below the saturation limit of adsorption sites.

As a consequence, a linear N_2 adsorption isotherm should be expected in the [0–1] bar pressure range. The above simulations suggest that Ca^{2+} cationic sites may not be equivalent toward N_2 molecules in the real zeolitic material as a competition would occur between adsorption sites involving different sorbant-sorbate interactions energies. One hypothesis for explaining the curvature of the experimental isotherm is related to the effective accessibility of Ca^{2+} cations in the real material. Experimentally, there is general agreement that the formation of hydroxyl groups in multivalent zeolites is due to hydrolysis by the cation and dissociation of the water molecule by the electric field created by the cation, leading to a decrease in the apparent charge of the Ca^{2+} cation. These simulations suggest a further experimental study concerning the influence of dehydration on the adsorption performances of the Ca-exchanged X-type zeolite.

CONCLUSION

In the present study, the ability of a simple interaction model, including Lennard-Jones and coulombic contributions, to provide significant simulations of silicalite and CaLSX adsorption properties towards N_2 and O_2 molecules has been examined, at 298 K and in the [0–1] bar pressure range. The GCMC calculations were successful in simulating silicalite adsorption properties in the whole [0–1] bar pressure range. The lack of N_2/O_2 selectivity in silicalite is clearly correlated to the uniformity of the sorbent surface. The adsorption phenomena is of a non specific nature, involving repulsive-dispersive interactions between N_2 or O_2 molecules and the oxygen atoms of the framework.

When dealing with the cation-containing CaLSX structure, obtaining quantitative results is a difficult task. The forcefield parameters involving framework oxygens determined from the study of silicalite could not be straightforwardly transferred to the CaLSX/sorbate systems. Their adjustment needed for fitting the experimental O_2 adsorption isotherm suggested an increase in atomic polarizability of oxygens of the framework from silicalite to CaLSX, which was at first related to the respective ionicity of both structures. The GCMC simulations, while failing in capturing the experimental N_2 adsorption isotherm in the whole [0–1] bar pressure range, give a good qualitative insight into the sorbate/sorbent interactions. The high N_2/O_2 selectivity is clearly correlated to the distribution of the Ca^{2+} cations within the supercage, as interactions between the quadrupolar N_2 molecules and the zeolitic surface are mainly of an electrostatic nature.

As a matter of fact, the results of GCMC calculations are dependant on both the structural model and the interaction model. Considering the large size of the system and the softness of the interactions involved in N_2 and O_2 adsorption phenomena, an accurate quantitative description of adsorption properties of this cationic zeolite probably requires more sophisticated forcefields and extended interaction models. Yet, in the specific case of the CaLSX zeolite, the simulations suggest that the effective accessibility of Ca^{2+} cations to adsorbed molecules may have an important role, therefore suggesting further experimental studies.

Using a simple model has proved to give significant insight into the experimental behaviour of both silicalite and CaLSX zeolites. In the particular field of the separation of N_2 and O_2 in zeolites, a molecular modeling approach enhances the fundamental understanding of the basic microscopic phenomena and is appropriate for establishing correlations between the microscopic features of the sorbent/sorbate systems and their macroscopic properties such as isotherms and adsorption heats. As it may be easily transferred to any zeolitic structure, our approach offers, especially in the perspective of industrial research, the possibility of being easily used by experimentalists and theoretical chemistry non specialists. In that respect, molecular modeling can be used as a complementary tool to experimental studies, as far as it succeeds in reproducing experimental tendancies and in yielding relevant molecular-level explanations of the macroscopic adsorption properties.

References

[1] Nicholson, D. (1996). "Using computer simulation to study the properties of molecules in micropores", *J. Chem. Soc., Faraday Trans.*, **92**(1), 1.

[2] Papai, I., Goursot, A., Fajula, F., Plee, D. and Weber, J. (1995). "Modeling of N_2 and O_2 adsorption in zeolites", *J. Phys. Chem.*, **99**, 12925.

[3] (a) London, F. (1940). *Zeit. Phys. Chem.*, **B11**, 222; (b) Slater, J. C. and Kirkwood, J. G. (1931). "The van der Waals forces in gases", *Phys. Rev.*, **37**, 682; (c) Müller, A. (1936). "The van der Waals potential and the lattice energy of a n-CH_2 chain molecule in a paraffin crystal", *Proc. Roy. Soc.*, **A154**, 624.

[4] Steele, W. (1993). "Molecular interactions for physical adsorption", *Chem. Rev.*, **93**, 2355.

[5] Van Köningsveld, H., Van Bekkum, H. and Jansen, J. C. (1987). "On the location of the tetrapropylammonium (TPA) ion in zeolite ZSM-5 with improved framework accuracy", *Acta Crystallogr.*, **B43**, 127.

[6] Goodbody, S. J., Watanabe, K., MacGowan, D., Walten, J. P. R. B. and Quirke, N. (1991). "Molecular simulation of methane and butane in silicalite", *J. Chem. Soc., Faraday Trans.*, **87**, 1951.

[7] Chiang, A. S., Dixon, A. G. and Ma, Y. H. (1984). "The determination of zeolite crystal diffusivity by gas chromatography. II-Experimental", *Chem. Eng. Sci.*, **39**, 1461; Papp, H., Hinsen, W., Do, N. T. and Baerns, M. (1984). "The adsorption of methane on H-ZSM-5 zeolite", *Thermochim. Acta*, **39**, 1461.

[8] Razmus, D. M. and Hall, C. K. (1991). "Prediction of gas adsorption in 5A zeolites using Monte Carlo simulation", *AIChE Journal*, **37**(5), 771.

[9] Murphy, C. S., Singer, K., Klein, M. L. and McDonald, I. R. (1980). "Pair wise additive effective potentials for nitrogen", *Molec. Physics*, **41**(6), 1387.

[10] Vitale, G., Bull, L. M., Morris, R. E., Cheetham, A. K., Toby, B. H., Coe, C. G. and MacDougall, J. E. (1995). "Combined neutron and X-ray powder diffraction study of zeolite CaLSX and a H_2-NMR study of its complex with benzene", *J. Phys. Chem.*, **99**, 16087.

[11] Pellenq, R. J. M. and Nicholson, D. N. (1994). "Intermolecular potential function for the physical adsorption of rare gases in silicalite", *J. Phys. Chem.*, **98**(50), 13347.

[12] Müller, U., Reichert, H., Robens, E., Unger, K. K., Grillet, Y., Rouquerol, F., Rouquerol, J. Pan, D., Mersmann, A. and Fresnius, Z. (1989). "High resolution sorption studies of argon and nitrogen on large crystals of microporous zeolite ZSM-5", *Fresenius Z. Anal. Chem.*, **333**, 433.

[13] Pellenq, R. J. M. (1994). *Ph. D. Thesis, Imperial College*, University of London.

[14] This work.